

# Septic pulmonary embolism caused by a *Klebsiella pneumoniae* liver abscess: clinical characteristics, imaging findings, and clinical courses

Deng-Wei Chou,<sup>1,\*</sup> Shu-Ling Wu,<sup>III</sup> Kuo-Mou Chung,<sup>I</sup> Shu-Chen Han<sup>II</sup>

<sup>I</sup>Tainan Municipal Hospital, Department of Internal Medicine, Division of Chest Medicine, Tainan/Taiwan. <sup>II</sup>Tainan Municipal Hospital, Department of Radiology, Tainan/Taiwan. <sup>III</sup>Chung-Hwa University of Medical Technology, Department of Long Term Care, Tainan/Taiwan.

**OBJECTIVES:** Septic pulmonary embolism caused by a *Klebsiella (K.) pneumoniae* liver abscess is rare but can cause considerable morbidity and mortality. However, clinical information regarding this condition is limited. This study was conducted to elucidate the full disease spectrum to improve its diagnosis and treatment.

**METHOD:** We reviewed the clinical characteristics, imaging findings, and clinical courses of 14 patients diagnosed with septic pulmonary embolism caused by a *K. pneumoniae* liver abscess over a period of 9 years.

**RESULTS:** The two most prevalent symptoms were fever and shortness of breath. Computed tomography findings included a feeding vessel sign (79%), nodules with or without cavities (79%), pleural effusions (71%), peripheral wedge-shaped opacities (64%), patchy ground-glass opacities (50%), air bronchograms within a nodule (36%), consolidations (21%), halo signs (14%), and lung abscesses (14%). Nine (64%) of the patients developed severe complications and required intensive care. According to follow-up chest radiography, the infiltrates and consolidations were resolved within two weeks, and the nodular opacities were resolved within one month. Two (14%) patients died of septic shock; one patient had metastatic meningitis, and the other had metastatic pericarditis.

**CONCLUSION:** The clinical presentations ranged from insidious illness with fever and respiratory symptoms to respiratory failure and septic shock. A broad spectrum of imaging findings, ranging from nodules to multiple consolidations, was detected. Septic pulmonary embolism caused by a *K. pneumoniae* liver abscess combined with the metastatic infection of other vital organs confers a poor prognosis.

**KEYWORDS:** Computed tomography; *Klebsiella pneumoniae*; Liver abscess; Septic pulmonary embolism.

Chou DW, Wu SL, Chung KM, Han SC. Septic pulmonary embolism caused by a *Klebsiella pneumoniae* liver abscess: clinical characteristics, imaging findings, and clinical courses. *Clinics*. 2015;70(6):400-407

Received for publication on November 3, 2014; First review completed on January 8, 2015; Accepted for publication on March 5, 2015

E-mail: choudw@gmail.com

\*Corresponding author

## INTRODUCTION

Septic pulmonary embolism (SPE) is a type of nonthrombotic pulmonary embolism in which a thrombus containing microorganisms causes an inflammatory reaction (1). SPE thrombi can cause pulmonary infarction and metastatic abscesses. SPE is a serious but rare condition that is challenging to diagnose. Because the clinical and radiographic features at presentation are not specific, the diagnosis of this disease is frequently delayed (2). Histopathological confirmation is typically unfeasible in clinical practice (2); thus, most SPE cases are diagnosed based on

computed tomography (CT) scan findings (2–5) and clinical evidence of infection (2). The typical CT scan findings that indicate SPE include peripheral nodules with or without cavitations, a feeding vessel sign, and wedge-shaped peripheral lesions abutting the pleura (3–5). In a systematic review of 168 SPE patients from June 1978 to September 2012, the most pervasive causative pathogen was *Staphylococcus aureus*, which accounted for 75 of 137 (55%) cases with positive blood cultures. *S. aureus* infections were frequent due to the use of intravenous drugs or an intravascular indwelling catheter or to the presence of soft tissue purulent infection. *Klebsiella (K.) pneumoniae* was the most prevalent causative gram-negative pathogen, accounting for 11 of 137 (8%) cases with positive blood cultures. Liver abscess was the most frequently observed primary source of infection in SPE caused by *K. pneumoniae* (6). A distinct type of invasive liver abscess syndrome caused by community-acquired *K. pneumoniae* was first reported in Taiwan in 1986 (7). During the previous two decades, this invasive liver abscess syndrome has been increasingly

**Copyright** © 2015 CLINICS – This is an Open Access article distributed under the terms of the Creative Commons Attribution Non-Commercial License (<http://creativecommons.org/licenses/by-nc/3.0/>) which permits unrestricted non-commercial use, distribution, and reproduction in any medium, provided the original work is properly cited.

No potential conflict of interest was reported.

**DOI:** 10.6061/clinics/2015(06)03



described in many countries (8–15) and has begun to emerge worldwide. Metastatic infection is a characteristic feature in this syndrome; the eyes, lungs, and central nervous system are the most common sites of metastasis (16,17).

In a nationwide population-based study in Taiwan, patients with a *K. pneumoniae* liver abscess (KPLA) had a consistently higher incidence of extrahepatic *K. pneumoniae* infection than patients without a liver abscess during the 1-year follow-up period. Among the extrahepatic *K. pneumoniae* infections, the incidence of SPE caused by a KPLA (SPE-KPLA) was 0.5% (18), and only a few cases of SPE-KPLA have been reported in the English-language literature (19–22). Although SPE-KPLA is rare, it can cause considerable morbidity (19,21,22) and mortality (19). However, the full spectrum of SPE-KPLA has not been well described. Therefore, this study was conducted to elucidate the clinical characteristics, imaging findings, and clinical courses of SPE-KPLA patients.

## MATERIALS AND METHODS

### Patient selection

The Institutional Review Board at our hospital approved this study. The study was conducted at the Tainan Municipal Hospital, a 516-bed referral teaching hospital in Southern Taiwan. We performed a computer-aided search of electronic medical records and an imaging database and identified 221 KPLA patients diagnosed between January 2005 and December 2013. Among the 221 patients, 14 had abnormal chest radiographic findings, including multiple nodular opacities (n=11) and ill-defined infiltrates (n=3). All 14 patients underwent a thoracic CT scan and follow-up chest radiography, and two of the 14 patients underwent a follow-up thoracic CT scan. The CT scans were obtained using two multidetector CT scanners at our institution, including a GE LightSpeed VCT 64-slice CT scanner (GE Healthcare, Milwaukee, USA) and a GE BrightSpeed Elite Select 16-slice CT scanner (GE Healthcare, Milwaukee, USA), during the 9-year period. The CT scanning parameters were as follows: 120 kV, 100 to 320 mA, 0.8-second rotation time, 5 mm slice thickness, and 5 mm interval. The images were reviewed at a lung window setting level of –700 Hounsfield units (HU) and width of 1500 HU and a mediastinum window setting level of 40 HU and a width of 350 HU. Two chest physicians (Chou DW and Chung KM) independently evaluated the thoracic CT findings and follow-up chest radiographs of the 14 patients. The thoracic CT findings included a feeding vessel sign, peripheral wedge-shaped opacity, nodules with or without cavities, patchy ground-glass opacities, air bronchograms within a nodule, consolidations, lung abscesses, halo signs, and pleural effusion. Any discrepancies were resolved by discussion with a chest radiologist (Han SC) to reach a final consensus. The following clinical data were collected from the 14 patients: gender, age, presented symptoms, comorbidities, laboratory data, antimicrobial susceptibilities, antibiotic therapy, surgical procedures, complications, length of stay, and outcomes.

The inclusion criteria for the diagnosis of SPE-KPLA were adapted from Cook et al. (2) and comprised (1) a CT scan showing multiple nodular opacities or ill-defined infiltrates compatible with SPE, (2) a KPLA serving as the primary source of infection, (3) clinical and radiographic improvement following antibiotic treatment, and (4) the exclusion of other potential explanations of lung lesions.

**Table 1** - Clinical characteristics, computed tomographic findings, and clinical courses of the 14 patients with septic pulmonary embolism caused by a *Klebsiella pneumoniae* liver abscess.

Variables	Value
<b>Clinical characteristics</b>	
Sex (male/female), n	10/4
Age (y), mean and range	59.6 ± 10.7 (39–80)
<b>Interval between SPE presentation and admission, n (%)</b>	
Day of admission	10 (71%)
≤ 3 days after admission	4 (29%)
<b>Presented symptoms, n (%)</b>	
Fever	14 (100%)
Shortness of breath	8 (57%)
Cough	5 (36%)
General weakness	5 (36%)
Altered mental status	2 (14%)
Hemoptysis	2 (14%)
Right upper quadrant abdominal pain	1 (7%)
<b>Comorbidities, n (%)</b>	
Diabetes mellitus	12 (86%)
Hypertension	2 (14%)
Cerebrovascular disease	1 (7%)
<b>Laboratory data, n (%)</b>	
White blood cell count > 10,000 cells/mm <sup>3</sup>	9 (64%)
Serum creatinine level > 1.5 mg/dL	8 (57%)
Serum alanine transaminase level > 40 IU/mL	6 (43%)
<b>Liver abscess location, n (%)</b>	
Right lobe	9 (64%)
Left lobe	4 (29%)
Both lobes	1 (7%)
<b>Computed tomographic findings</b>	
Feeding vessel sign	11 (79%)
Nodule	
Without cavity	11 (79%)
With cavity	11 (79%)
Peripheral wedge-shaped opacity	9 (64%)
Patchy ground-glass opacity	7 (50%)
Air bronchograms within a nodule	5 (36%)
Focal consolidation	3 (21%)
Halo sign	2 (14%)
Lung abscess	2 (14%)
Pleural effusion	
Bilateral	4 (29%)
Right	4 (29%)
Left	2 (14%)
Lesions in	
Bilateral lungs	12 (86%)
Right lung	2 (14%)
<b>Clinical courses</b>	
Antibiotic therapy, n (%)	
Ceftriaxone combined with metronidazole	10 (71%)
Carbapenem	3 (21%)
Piperacillin/tazobactam	1 (7%)
Surgical procedures, n (%)	
Pigtail catheter drainage of liver abscess	10 (71%)
Tube thoracostomy	2 (14%)
Video-assisted thoracostomy with decortication	1 (7%)
Complications, n (%)	
Acute kidney injury	8 (57%)
Septic shock	6 (43%)
Acute respiratory failure	5 (36%)
Length of stay in hospital (d), mean and range	20.9 ± 21.1 (8–42)
Mortality, n (%)	2 (14%)

### Definitions

A case of KPLA was defined as the presence of one or multiple liver abscesses detected by sonography or CT as well as culture-confirmed *K. pneumoniae* isolated from a liver



abscess aspirate or the blood. The diagnostic criteria for acute kidney injury included an increase in serum creatinine by at least 0.3 mg/dL within 48 hours (23). Halo sign was defined as a ground-glass attenuation surrounding a pulmonary nodule on the CT scan (24). Ground-glass opacity was defined as a hazy increase in attenuation without the obscuration of vascular markings. Consolidation was defined as a localized increase in lung attenuation with the obscuration of vascular markings.

## RESULTS

### Clinical characteristics

We identified 14 patients with SPE-KPLA. Table 1 lists the clinical characteristics, CT findings, and clinical courses of the 14 patients with SPE-KPLA, all of whom were admitted through the emergency department. Liver abscess with SPE was diagnosed on the day of admission in 10 (71%) of the patients and within 3 days of admission in the remaining 4 (29%) patients. Diabetes mellitus was the major underlying disease (n=12). Of the 12 (83%) diabetic patients, 10 exhibited a glycosylated hemoglobin value higher than 12%, 5 presented with hyperosmolar hyperglycemia syndrome, and one presented with diabetic ketoacidosis upon admission. Among the 14 patients, the 2 most prevalent symptoms were fever and

shortness of breath. Most patients had an elevated white blood cell count and serum creatinine level. Gas formation in the abscess was observed in 5 (36%) of the patients.

### Imaging findings

More than two imaging findings were identified for each patient, and 12 (86%) of the patients exhibited lesions in both lungs. The most common CT findings were a feeding vessel sign (Figure 1A), peripheral wedge-shaped opacity (Figure 1B), a nodule with or without a cavity (Figure 1A), and patchy ground-glass opacities (Figure 2A). Other CT findings included air bronchograms within a nodule (Figure 2B), focal consolidations (Figure 3), lung abscesses (Figure 1A), and halo signs (Figure 1B). Pleural effusion was observed in 10 (71%) of the patients. Two patients who underwent a follow-up thoracic CT scan; one exhibited new lung abscess formation (Figures 4A-B), and the second exhibited new loculated pleural effusion formation (Figures 4C-D). Among the 12 survivors, follow-up chest radiography revealed that 7 patients had ill-defined infiltrates that were resolved within 7–14 days and 8 patients had nodular opacities that were resolved within 10–30 days.

### Clinical courses

Community-acquired *K. pneumoniae* bacteremia was confirmed in all 14 patients. All 38 *K. pneumoniae* isolates

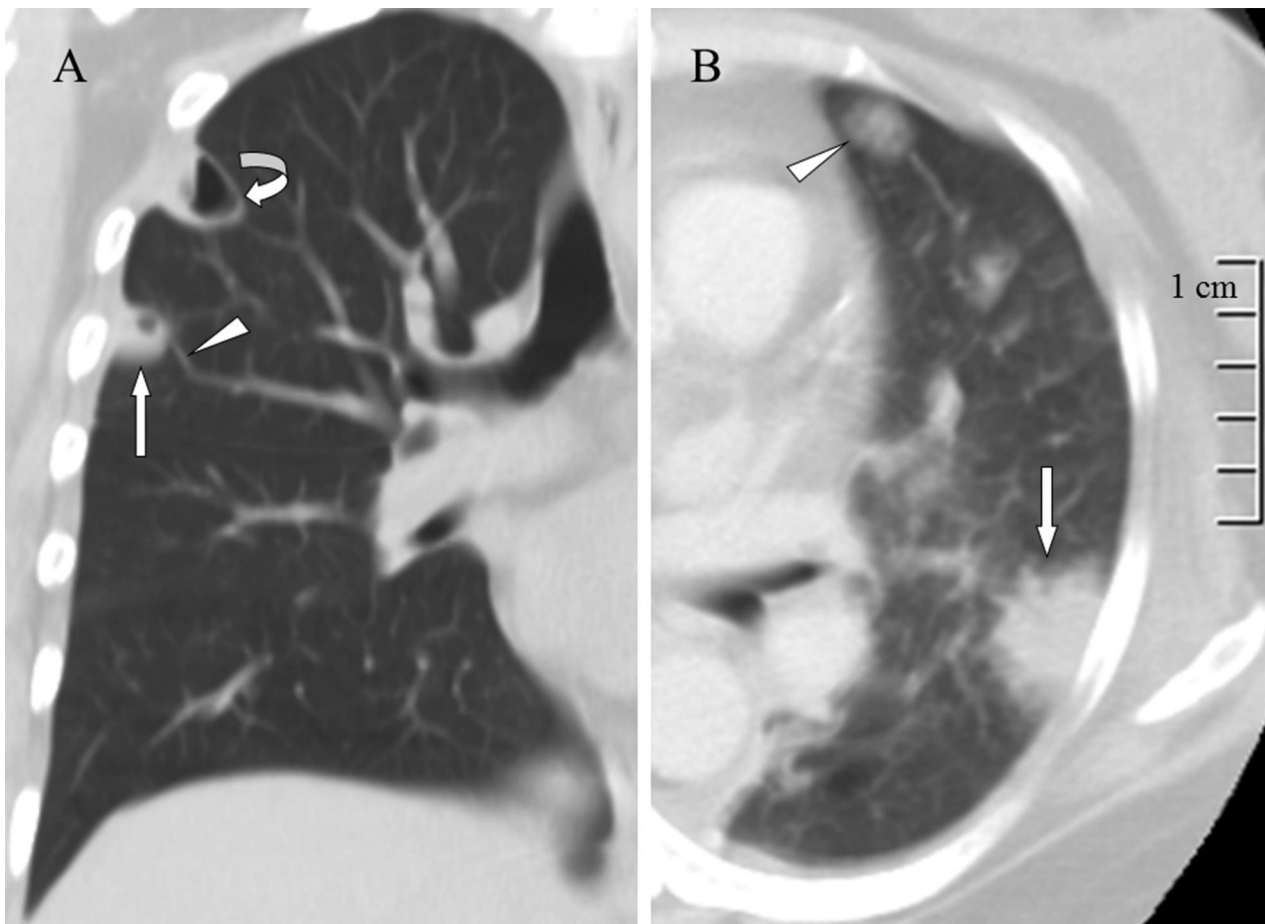


**Figure 1 - A)** A lung window of a coronal computed tomography scan shows a cavitary nodule (arrow) with a feeding vessel sign (arrowhead) and lung abscess (curved arrow) in the right upper lobe. **B)** A lung window of a cross-sectional computed tomography scan shows a peripheral wedge-shaped opacity (arrow) and ground-glass attenuation surrounding a pulmonary nodule (arrowhead) in the left upper lobe.

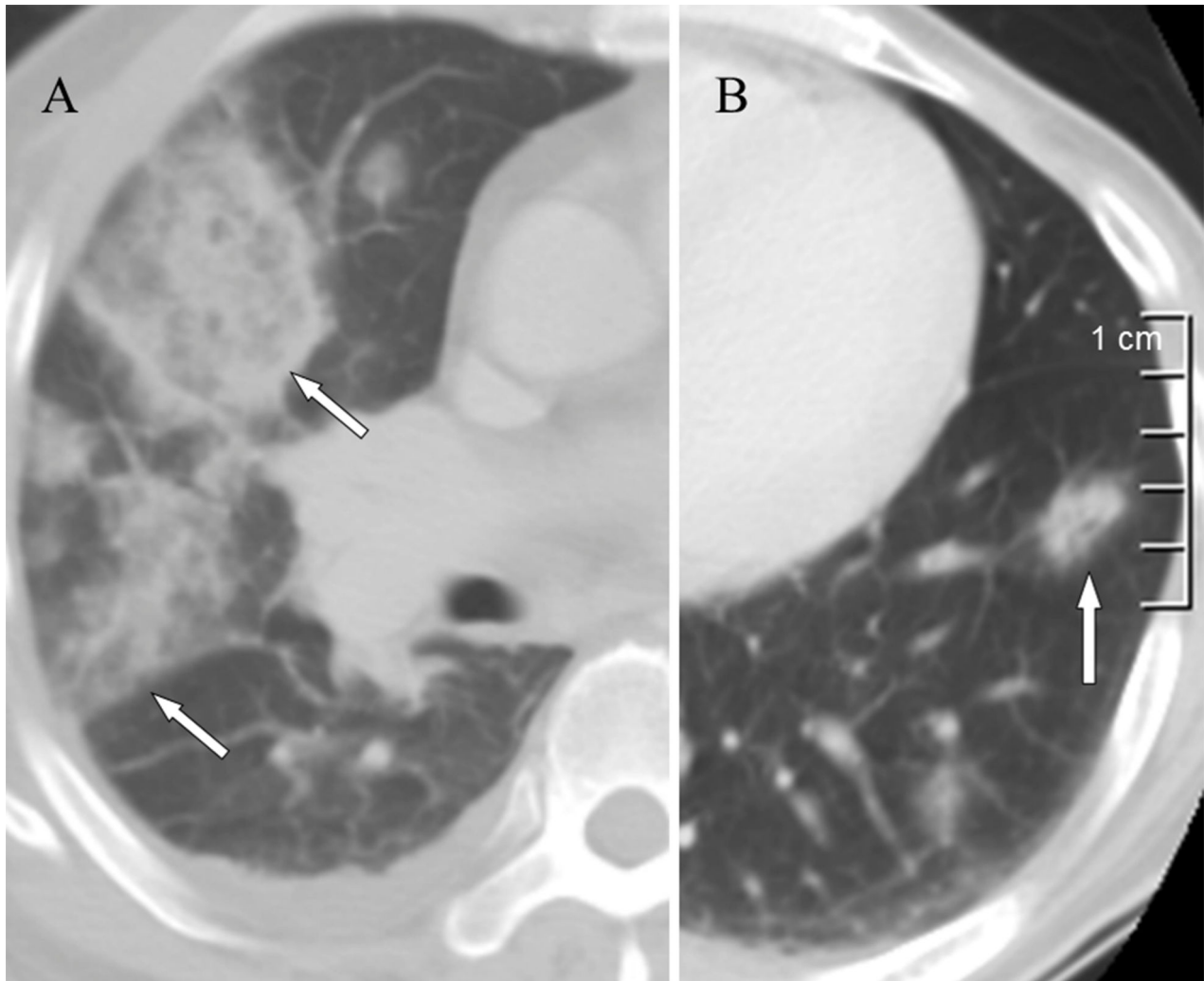


**Figure 2 - A)** A lung window of a cross-sectional computed tomography scan shows multiple patchy ground-glass opacities (arrows) in the right lung. **B)** A lung window of a cross-sectional computed tomography scan shows air bronchograms within a nodule (arrow) in the left lung.

(28 from the blood and 10 from liver abscess aspirates) were susceptible to cephalosporins, aminoglycosides, carbapenem, and levofloxacin. Six isolates (4 from the blood and 2 from liver abscess aspirates) from two of the patients were resistant to ampicillin/sulbactam. Three isolates (2 from the blood and one from a liver abscess aspirate) from one of the patients were resistant to piperacillin. All 38 isolates expressed the hypermucoviscous phenotype. Bacterial cultures of sputum (n=9) or endotracheal aspirates (n=5) showed negative results. Antibiotic therapy was initiated on the day of admission and was administered for 2–6 weeks.

Among the 14 patients, 10 underwent pigtail catheter drainage of the liver abscess, 4 had an immature liver abscess and did not receive drainage, 2 had massive pleural effusions, one had a loculated pleural effusion that occurred one week after SPE treatment, two underwent tube thoracostomy for massive pleural effusions, and one underwent video-assisted thoracostomy with decortications for a loculated pleural effusion. The pleural effusions of the three patients were serosanguinous in appearance and were exudates predominated by neutrophils.

Nine (64%) patients developed severe complications, including acute kidney injury, septic shock, and acute respiratory failure, within 7 days of SPE presentation and were admitted to the intensive care unit (ICU). The mean Acute Physiologic and Chronic Health Evaluation II score during the first 24 hours after ICU admission was 14 (range: 10 to 20). The mean ICU length of stay was  $15.5 \pm 12.2$  days. Two patients died during hospitalization, representing an in-hospital mortality of 14%. These two patients died of refractory shock; one had septic metastatic meningitis, and the other had septic metastatic pericarditis (Figures 5A-C). The follow-up duration of the 12 survivors after hospital discharge ranged from 3 to 48 months, and none of the survivors had complications resulting from SPE-KPLA.

## DISCUSSION

In this study, SPE-KPLA was diagnosed in 14 of the 221 (6%) patients, which is consistent with the rate of 4.5% (5 of 110 patients) reported by a previous study (16). However, several tiny nodules were not observed in chest radiographs and were only detected in thoracic CT scans. Therefore, the



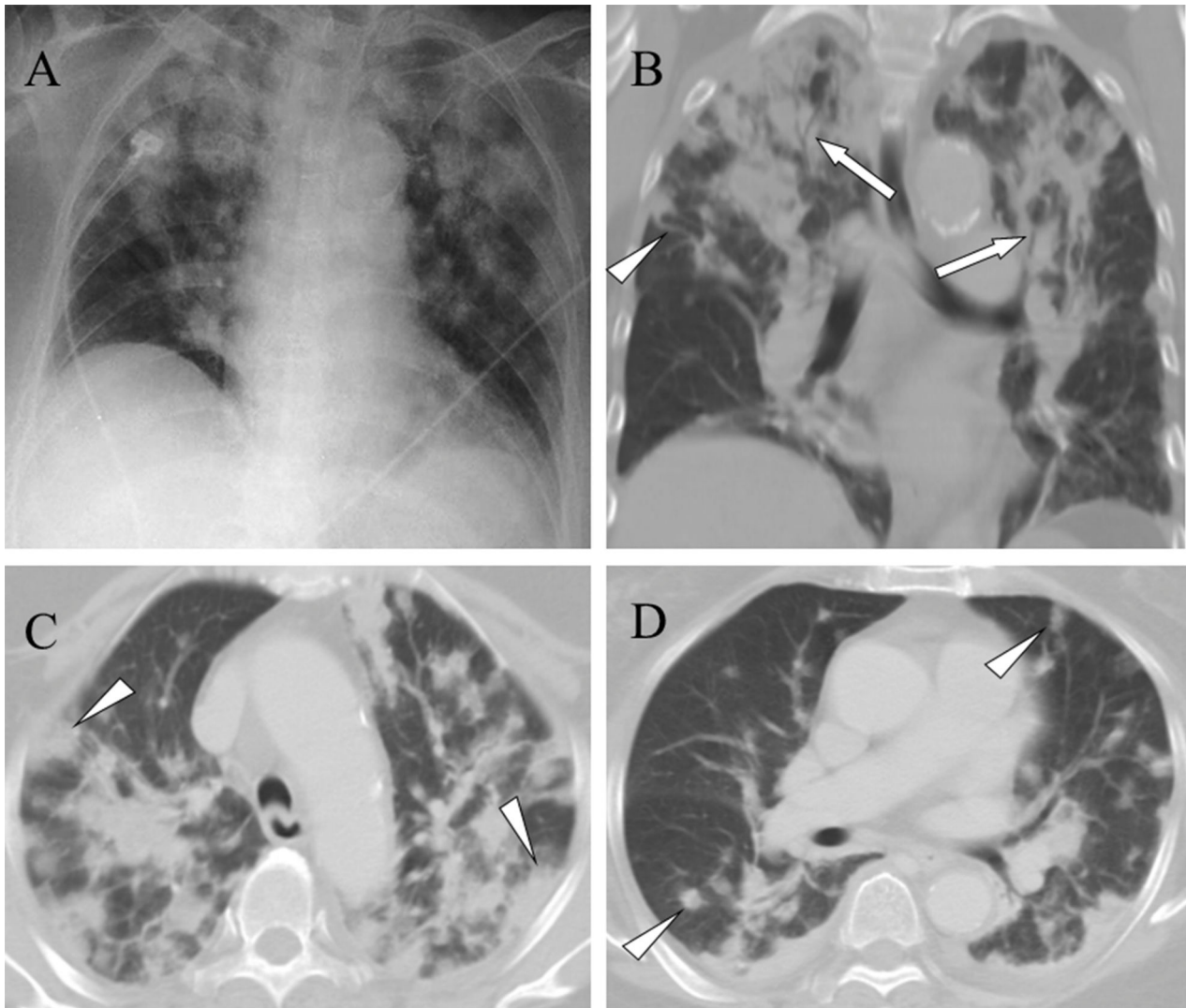


**Figure 3 - A)** A chest radiograph reveals multiple alveolar consolidations, predominantly in the upper lung zones. **B)** A lung window of a coronal computed tomography scan shows multiple consolidations with air bronchograms (arrows) in the upper lobes. Additionally, a nodule with a feeding vessel sign (arrowhead) is shown. **C)** A lung window of a cross-sectional computed tomography scan shows multiple peripheral wedge-shaped (arrowheads) and **D)** nodular (arrowheads) opacities in the bilateral lungs.

prevalence of SPE-KPLA may have been underestimated because thoracic CT scans were performed only on the 14 patients with abnormal chest radiographic findings.

Among the 12 diabetic SPE-KPLA patients, 10 (83%) exhibited glycosylated hemoglobin values higher than 12%, indicating that poor glycemic control was highly associated with septic metastatic infection. The two most prevalent symptoms were fever and shortness of breath. Only one patient complained of abdominal pain upon admission. The absence of abdominal pain was likely due to hypoesthesia caused by diabetic polyneuropathy. Establishing an SPE-KPLA diagnosis in diabetic patients can be challenging without pathognomonic physical findings. Thus, a high index of suspicion is crucial for early recognition. When diabetic patients present with fever and shortness of breath, and abnormal chest radiograph findings reveal multiple nodular opacities and ill-defined infiltrate patterns, abdominal sonography should be performed to eliminate the possibility of a liver abscess. Additionally, 70% of the SPEs were present upon admission, and 30% occurred within

3 days of admission, indicating that SPEs can occur fulminantly. New SPE formation occurred despite performing broad-spectrum antibiotic therapy and pigtail catheter drainage of the liver abscess for more than one week, indicating that SPEs could not be prevented.

All *K. pneumoniae* isolates were susceptible to cephalosporins, aminoglycosides, and levofloxacin, and susceptibility to ampicillin/sulbactam and piperacillin varied. No nosocomial or multiresistant strains were identified. In this study, which examined patients treated between 2005 and 2013, the pattern of antimicrobial susceptibility was similar to that reported by a previous study involving patients treated between 1990 and 1996 (8). Remarkably, the antimicrobial susceptibility pattern of *K. pneumoniae*, which causes community-acquired liver abscesses, has remained unchanged in Taiwan over the past 20 years. This is the case because the *K. pneumoniae* strain that causes liver abscesses is community-acquired and is not naturally a multiresistant strain (8). In this study, all *K. pneumoniae* isolates expressed the hypermucoviscous phenotype. Hypermucoviscosity has

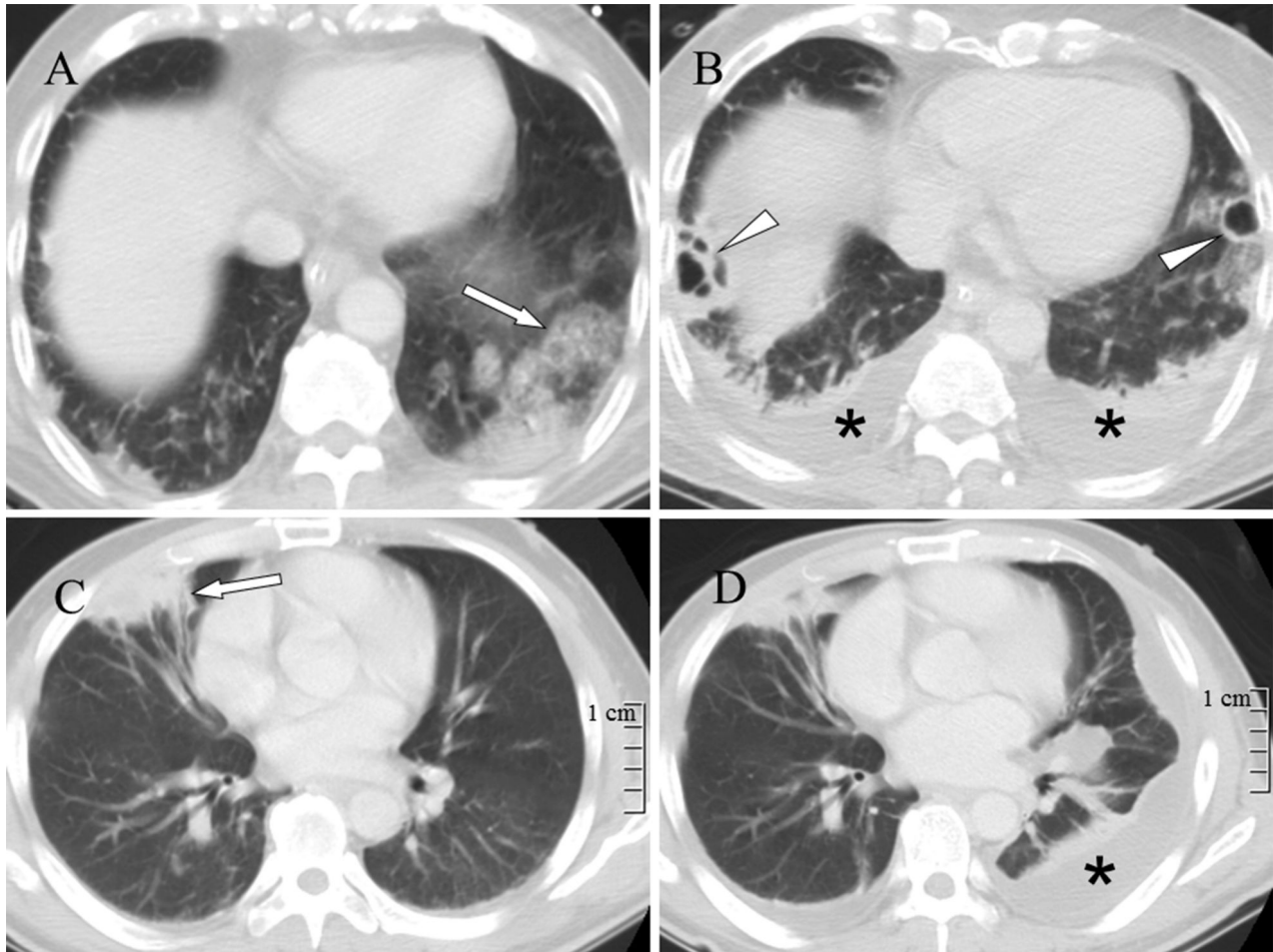


**Figure 4 - A)** A lung window of a cross-sectional computed tomography scan shows patchy ground-glass opacities in the left lower lobe (arrow). **B)** A repeat computed tomography scan obtained in the same image plane 7 days later shows new bilateral lung abscess (arrowheads) and pleural effusion (asterisks) formation. **C)** A lung window of a cross-sectional computed tomography scan shows a peripheral wedge-shaped opacity in the right middle lobe (arrow). **D)** A repeat computed tomography scan obtained in the same image plane 12 days later shows interval regression of the peripheral wedge-shaped opacity. A new left loculated pleural effusion (asterisk) formation is observed.

been correlated with a high level of resistance to complement-mediated serum killing (25). The hypermucoviscous phenotype of *K. pneumoniae* bacteremic isolates has been associated with the development of a distinctive invasive syndrome (26). The hypermucoviscous phenotype of the capsular serotype K1 has been reported as a major virulence factor of *K. pneumoniae* that causes primary liver abscess and septic metastatic complications (27,28). Clinicians should therefore initiate aggressive investigations for invasive diseases when the hypermucoviscous phenotype is identified.

In this study, protean presentations of SPE-KPLA ranged from insidious illness with fever and respiratory symptoms such as shortness of breath, cough, and hemoptysis to respiratory failure and septic shock. Among the nine patients who required ICU care, seven patients recovered without septic metastasis to other vital organs, and two patients died from septic metastasis to other vital organs; one of the patients had septic metastatic meningitis and died on Day 42 following admission as a result of refractory shock and multiple organ failure, and the other had septic metastatic pericarditis without cardiac tamponade and died on Day 8 following admission due to refractory shock. Thus, SPE

combined with metastatic infection of other vital organs confers a poor prognosis.

In SPE, the microembolism is not directly observed on CT images, and diagnosis relies on lung parenchymal findings. Indirect signs of SPE include pulmonary edema, infarction, empyema, and pulmonary hypertension (1). In this study, a broad spectrum of CT findings was detected, varying from nodules to multiple consolidations. Typical CT findings indicative of SPE-KPLA included peripheral nodules with or without cavities, a feeding vessel sign, and peripheral wedge-shaped opacities, all of which have been previously reported (18–21). However, previous studies have not comprehensively described the halo sign, patchy ground-glass opacities, and multiple focal consolidations in SPE-KPLA. The halo sign pathologically represents hemorrhagic pulmonary nodules, tumor cell infiltration, or nonhemorrhagic inflammatory lesions. Hemorrhagic pulmonary nodules may occur in infectious diseases, including invasive pulmonary aspergillosis, mucormycosis, and candidiasis (29). Although a halo sign is not specific, it enables most hemorrhagic pulmonary nodules to be distinguished from nonhemorrhagic nodules (30,31). Ground-glass opacities

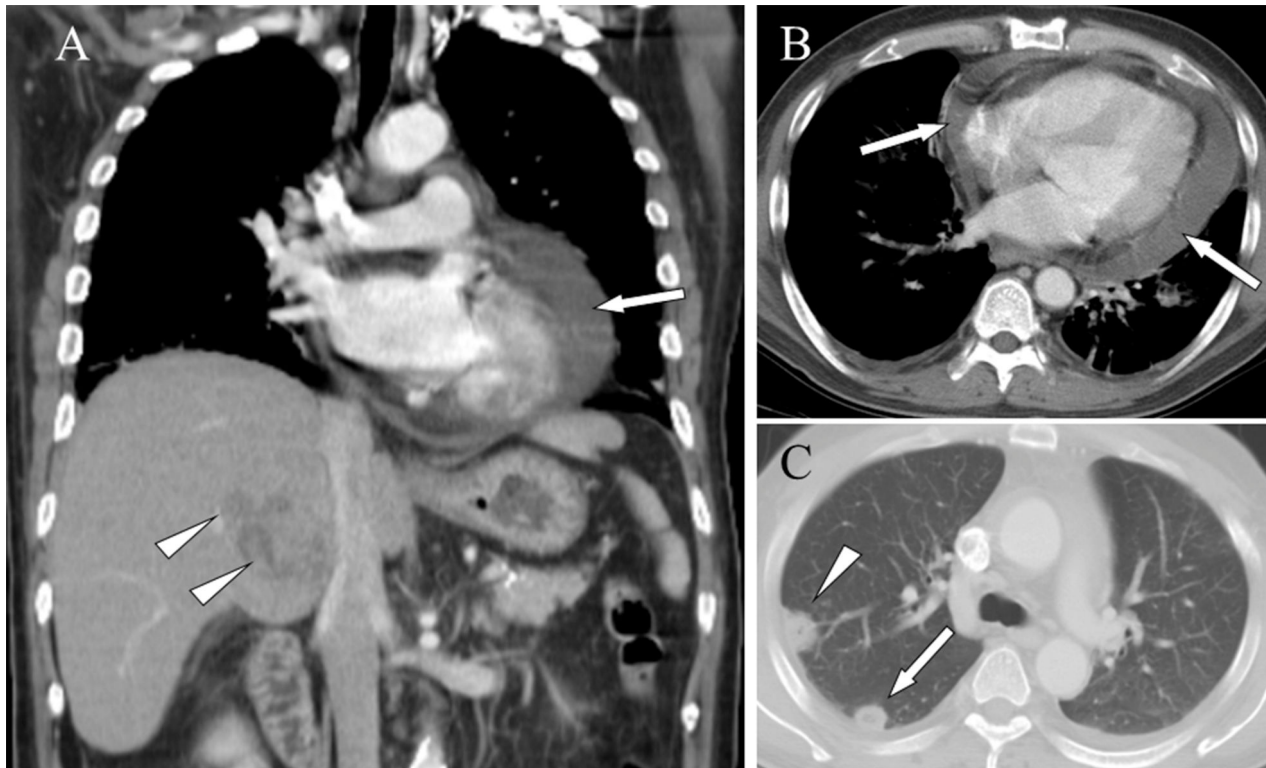


**Figure 5** - Pericardial effusion and septic pulmonary embolism caused by a *Klebsiella pneumoniae* liver abscess in a 73-year-old woman. **A)** A mediastinum window of a coronal computed tomography scan reveals a hypodense, hypovascular mass of approximately 5 cm in diameter in the S7 area of the right hepatic lobe (arrowheads) and fluid in the pericardial space (arrow). **B)** A mediastinum window of a cross-sectional computed tomography scan shows fluid in the pericardial space (arrows). **C)** A lung window of a cross-sectional computed tomography scan shows a peripheral wedge-shaped (arrowhead) and a peripheral nodular (arrow) opacity.

may be caused by alveolar hemorrhage, cytomegalovirus pneumonia, *Pneumocystis carinii* pneumonia, and bronchiolitis obliterans with organizing pneumonia (32). The presence of parenchymal consolidation in pulmonary infarction is primarily caused by pulmonary hemorrhage (33). The endothelial cells of the capillaries and arterioles as well as the venules of the lungs are highly susceptible to hypoxia. Therefore, mild transient ischemia of lung tissue may result in marked vessel dilation as well as increased vascular permeability with fluid and erythrocyte leakage (34). In this study, hemoptysis was observed in patients with CT findings revealing patchy ground-glass opacities and multiple focal consolidations indicating pulmonary hemorrhage.

Two limitations were encountered while conducting this study. First, we retrospectively evaluated only those patients who underwent thoracic CT scans, which may have resulted in selection bias. Additionally, because the patient sample was relatively small, we could not identify statistically significant predictors of mortality. A larger sample is required to generalize our findings with greater confidence (although SPE-KPLA cases remain exceptionally rare). Second, no histopathological confirmation was associated with the CT findings. Because histopathological confirmation was unfeasible, the current SPE diagnosis was based on CT findings and clinical evidence of infection. Despite this shortcoming, we believe that the CT findings and subsequent clinical courses allowed the diagnosis to be made with confidence.

The main findings of this study are summarized as follows. First, the clinical presentations ranged from

insidious illness with fever and respiratory symptoms to respiratory failure and septic shock. Second, a broad spectrum of imaging findings was detected, ranging from nodules to multiple consolidations. Finally, SPE-KPLA combined with the metastatic infection of other vital organs poses a poor prognosis.

#### ■ AUTHOR CONTRIBUTIONS

Chou DW designed the study, interpreted the clinical data, and wrote the manuscript. Wu SL collected and analyzed the clinical data. Chou DW, Chung KM, and Han SC evaluated the chest radiographs and CT scans.

#### ■ REFERENCES

- Bach AG, Restrepo CS, Abbas J, Villanueva A, Lorenzo Dus MJ, Schöpf R, et al. Imaging of nonthrombotic pulmonary embolism: biological materials, nonbiological materials, and foreign bodies. *Eur J Radiol.* 2013;82(3):e120-41, <http://dx.doi.org/10.1016/j.ejrad.2012.09.019>.
- Cook RJ, Ashton RW, Aughenbaugh GL, Ryu JH. Septic pulmonary embolism: presenting features and clinical course in 14 patients. *Chest.* 2005;128(1):162-6, <http://dx.doi.org/10.1378/chest.128.1.162>.
- Kuhlman JE, Fishman EK, Teigen C. Pulmonary septic emboli: diagnosis with CT. *Radiology.* 1990;174(1):211-3, <http://dx.doi.org/10.1148/radiology.174.1.2294550>.
- Huang RM, Naidich DP, Lubat E, Schinella R, Garay SM, McCauley DI. Septic pulmonary emboli: CT-radiographic correlation. *AJR Am J Roentgenol.* 1989;153(1):41-5, <http://dx.doi.org/10.2214/ajr.153.1.41>.
- Iwasaki Y, Nagata K, Nakanishi M, Natuhara A, Harada H, Kubota Y, et al. Spiral CT findings in septic pulmonary emboli. *Eur J Radiol.* 2001;37(3):190-4, [http://dx.doi.org/10.1016/S0720-048X\(00\)00254-0](http://dx.doi.org/10.1016/S0720-048X(00)00254-0).
- Ye R, Zhao L, Wang C, Wu X, Yan H. Clinical characteristics of septic pulmonary embolism in adults: a systematic review. *Respir Med.* 2014;108(1):1-8, <http://dx.doi.org/10.1016/j.rmed.2013.10.012>.





7. Liu YC, Cheng DL, Lin CL. Klebsiella pneumoniae liver abscess associated with septic endophthalmitis. *Arch Intern Med.* 1986;146(10):1913–6, <http://dx.doi.org/10.1001/archinte.1986.00360220057011>.
8. Wang JH, Liu YC, Lee SS, Yen MY, Chen YS, Wang JH, et al. Primary liver abscess due to Klebsiella pneumoniae in Taiwan. *Clin Infect Dis.* 1998;26(6):1434–8, <http://dx.doi.org/10.1086/cid.1998.26.issue-6>.
9. Siu LK, Yeh KM, Lin JC, Fung CP, Chang FY. Klebsiella pneumoniae liver abscess: a new invasive syndrome. *Lancet Infect Dis.* 2012;12(11):881–7, [http://dx.doi.org/10.1016/S1473-3099\(12\)70205-0](http://dx.doi.org/10.1016/S1473-3099(12)70205-0).
10. Chung DR, Lee SS, Lee HR, Kim HB, Choi HJ, Eom JS, et al. and Korean Study Group for Liver Abscess. Emerging invasive liver abscess caused by K1 serotype Klebsiella pneumoniae in Korea. *J Infect.* 2007;54(6):578–83, <http://dx.doi.org/10.1016/j.jinf.2006.11.008>.
11. Lederman ER, Crum NF. Pyogenic liver abscess with a focus on Klebsiella pneumoniae as a primary pathogen: an emerging disease with unique clinical characteristics. *Am J Gastroenterol.* 2005;100(2):322–31, <http://dx.doi.org/10.1111/ajg.2005.100.issue-2>.
12. Pope JV, Teich DL, Clardy P, McGillicuddy DC. Klebsiella pneumoniae liver abscess: an emerging problem in North America. *J Emerg Med.* 2011;41(5):e103–5, <http://dx.doi.org/10.1016/j.jemermed.2008.04.041>.
13. Anstey JR, Fazio TN, Gordon DL, Hogg G, Jenney AW, Maiwald M, et al. Community-acquired Klebsiella pneumoniae liver abscesses – an “emerging disease” in Australia. *Med J Aust.* 2010;193(9):543–5.
14. Moore R, O’Shea D, Geoghegan T, Mallon PW, Sheehan G. Community-acquired Klebsiella pneumoniae liver abscess: an emerging infection in Ireland and Europe. *Infection.* 2013;41(3):681–6, <http://dx.doi.org/10.1007/s15010-013-0408-0>.
15. Sachdev DD, Yin MT, Horowitz JD, Mukkamala SK, Lee SE, Ratner AJ. Klebsiella pneumoniae K1 liver abscess and septic endophthalmitis in a U.S. resident. *J Clin Microbiol.* 2013;51(3):1049–51, <http://dx.doi.org/10.1128/JCM.02853-12>.
16. Lee SS, Chen YS, Tsai HC, Wann SR, Lin HH, Huang CK, et al. Predictors of septic metastatic infection and mortality among patients with Klebsiella pneumoniae liver abscess. *Clin Infect Dis.* 2008;47(5):642–50, <http://dx.doi.org/10.1086/592125>.
17. Fang CT, Lai SY, Yi WC, Hsueh PR, Liu KL, Chang SC. Klebsiella pneumoniae genotype K1: an emerging pathogen that causes septic ocular or central nervous system complications from pyogenic liver abscess. *Clin Infect Dis.* 2007;45(3):284–93, <http://dx.doi.org/10.1086/519262>.
18. Keller JJ, Tsai MC, Lin CC, Lin YC, Lin HC. Risk of infections subsequent to pyogenic liver abscess: a nationwide population-based study. *Clin Microbiol Infect.* 2013;19(8):717–22, <http://dx.doi.org/10.1111/1469-0691.12027>.
19. Yang PW, Lin HD, Wang LM. Pyogenic liver abscess associated with septic pulmonary embolism. *J Chin Med Assoc.* 2008;71(9):442–7, [http://dx.doi.org/10.1016/S1726-4901\(08\)70146-1](http://dx.doi.org/10.1016/S1726-4901(08)70146-1).
20. Lee SJ, Cha SI, Kim CH, Park JY, Jung TH, Jeon KN, et al. Septic pulmonary embolism in Korea: Microbiology, clinicoradiologic features, and treatment outcome. *J Infect.* 2007;54(3):230–4, <http://dx.doi.org/10.1016/j.jinf.2006.04.008>.
21. Hagiya H, Kuroe Y, Nojima H, Otani S, Sugiyama J, Naito H, et al. Emphysematous liver abscesses complicated by septic pulmonary emboli in patients with diabetes: two cases. *Intern Med.* 2013;52(1):141–5, <http://dx.doi.org/10.2169/internalmedicine.52.8737>.
22. Zenda T, Araki I, Hiraiwa Y, Miyayama S, Masunaga T, Takeda Y, et al. Septic pulmonary emboli secondary to pyogenic liver abscess in a diabetic patient. *Intern Med.* 1995;34(1):42–5, <http://dx.doi.org/10.2169/internalmedicine.34.42>.
23. Mehta RL, Kellum JA, Shah SV, Molitoris BA, Ronco C, Warnock DG, et al. and Acute Kidney Injury Network. Acute Kidney Injury Network: report of an initiative to improve outcomes in acute kidney injury. *Crit Care.* 2007;11(2):R31, <http://dx.doi.org/10.1186/cc5713>.
24. Gaeta M, Blandino A, Scribano E, Minutoli F, Volta S, Pandolfo I. Computed tomography halo sign in pulmonary nodules: frequency and diagnostic value. *J Thorac Imaging.* 1999;14(2):109–13, <http://dx.doi.org/10.1097/00005382-199904000-00008>.
25. Fang CT, Chuang YP, Shun CT, Chang SC, Wang JT. A novel virulence gene in Klebsiella pneumoniae strains causing primary liver abscess and septic metastatic complications. *J Exp Med.* 2004;199(5):697–705, <http://dx.doi.org/10.1084/jem.20030857>.
26. Lee HC, Chuang YC, Yu WL, Lee NY, Chang CM, Ko NY, et al. Clinical implications of hypermucoviscosity phenotype in Klebsiella pneumoniae isolates: association with invasive syndrome in patients with community-acquired bacteraemia. *J Intern Med.* 2006;259(6):606–14, <http://dx.doi.org/10.1111/jim.2006.259.issue-6>.
27. Fang CT, Lai SY, Yi WC, Hsueh PR, Liu KL, Chang SC. Klebsiella pneumoniae genotype K1: an emerging pathogen that causes septic ocular or central nervous system complications from pyogenic liver abscess. *Clin Infect Dis.* 2007;45(3):284–93, <http://dx.doi.org/10.1086/519262>.
28. Fung CP, Chang FY, Lee SC, Hu BS, Kuo BI, Liu CY, et al. A global emerging disease of Klebsiella pneumoniae liver abscess: is serotype K1 an important factor for complicated endophthalmitis? *Gut.* 2002;50(3):420–4, <http://dx.doi.org/10.1136/gut.50.3.420>.
29. Kim Y, Lee KS, Jung KJ, Han J, Kim JS, Suh JS. Halo sign on high resolution CT: findings in spectrum of pulmonary diseases with pathologic correlation. *J Comput Assist Tomogr.* 1999;23(4):622–6, <http://dx.doi.org/10.1097/00004728-199907000-00025>.
30. Lee YR, Choi YW, Lee K, Jeon SC, Park CK, Heo JN. CT halo sign: the spectrum of pulmonary diseases. *Br J Radiol.* 2005;78(933):862–5, <http://dx.doi.org/10.1259/bjr/77712845>.
31. Primack SL, Hartman TE, Lee KS, Müller NL. Pulmonary nodules and the CT halo sign. *Radiology.* 1994;190(2):513–5, <http://dx.doi.org/10.1148/radiology.190.2.8284408>.
32. Worthy SA, Flint JD, Müller NL. Pulmonary complications after bone marrow transplantation: high-resolution CT and pathologic findings. *Radiographics.* 1997;17(6):1359–71, <http://dx.doi.org/10.1148/radiographics.17.6.9397451>.
33. Balakrishnan J, Meziane MA, Siegelman SS, Fishman EK. Pulmonary infarction: CT appearance with pathologic correlation. *J Comput Assist Tomogr.* 1989;13(6):941–5, <http://dx.doi.org/10.1097/00004728-198911000-00001>.
34. Wagenvoort CA. Pathology of pulmonary thromboembolism. *Chest.* 1995;107(1 Suppl):10S–17S.